Attack-resilient Distributed Control for Islanded Single-/three-phase Microgrids Based on Distributed Adaptive Observers

Jianguo Zhou, *Member*, *IEEE*, Yinliang Xu, *Senior Member*, *IEEE*, Lun Yang, *Student Member*, *IEEE*, and Hongbin Sun, *Fellow*, *IEEE*

***Abstract*—This paper investigates the power sharing and voltage regulation issues of islanded single-/three-phase microgrids (S/T-MGs) where both sources and loads are unbalanced and the presence of adversarial cyber-attacks against sensors of distributed generator (DG) units is considered. Firstly, each DG unit is modeled as a heterogeneous linear dynamic agent with disturbances caused by sources and loads, then the problem is formulated as a distributed containment control problem. After that, to guarantee satisfactory power sharing and voltage control performance asymptotically achieved for the S/T-MGs, an attack-resilient distributed secondary control approach is developed by designing a distributed adaptive observer. With this approach, the effect of the cyber-attacks can be neutralized to ensure system stability and preserve bounded voltage synchronization. Simulation results are presented to demonstrate the effectiveness of the proposed control approach.**

***Index Terms*—Single-/three-phase microgrid, cyber-attack, resilient distributed control, distributed observer, power sharing.**

I. Introduction

LOAD power sharing, voltage and frequency regulation are the most important issues in microgrids (MGs), which have been widely studied [1], [2]. However, the MG is usually characterized by unbalance [3]-[6] due to the integration of single-phase distributed generators (SDGs)/loads and the occurrence of asymmetrical faults, challenging the secure and reliable operation of the unbalanced single-/three-phase MGs (S/T-MGs).

For the topic of power sharing in unbalanced MGs, various research works have been reported [3], [5]-[9] and therein. Unlike the conventional centralized [9] and decentralized [5]-[7] control methods, distributed control is a popular control fashion now. For example, in the area of integrated energy systems (IESs), distributed approaches have been explored [10]-[12]. In 2019, Li *et al.* [10] first proposed an event-triggered based distributed gradient algorithm to solve the multi-timescale energy management problem for multi-energy system, which makes outstanding contributions to achieving the paradigm shift of energy management from single-timescale to multi-timescale with fully distributed implantation. In the context of MGs, in our previous work [3], a distributed method was proposed to realize proportional harmonic and imbalance power sharing among DGs. However, only unbalanced loads connected to the common bus are considered, and unbalanced sources such as hybrid SDGs and three-phase DGs (TDGs) are not included. Regarding this scenario, an event-based distributed approach was proposed in [13] to balance the output power of TDGs. However, similar to [6], [7], extra equipments are required. Voltage control along with power quality improvement is another equally important problem in unbalanced MGs. Besides centralized approaches [14], [15], distributed approaches have also been proposed. For example, Meng *et al.* [16] proposed a distributed method used for voltage unbalance compensation, where, however, only unbalanced loads are considered. Therefore, centralized [17], [18] and master-slave approaches [19] were, respectively, developed to improve the voltage quality only using SDGs without coordination with TDGs. Burgos-Mellado *et al.* [20] proposed a distributed cooperative control scheme based on the conservative power theory to share the unbalanced and distorted components of the currents and powers and to regulate the maximum voltage imbalance/distortion at the point of common coupling (PCC). Nevertheless, these research works still only discuss the scenario of unbalanced loads. To the best of the authors' knowledge, only [21] considers the cooperation of SDGs and TDGs for unbalance compensation and balance operation of TDGs. Moreover, when considering unbalanced sources, the conventional droop control [1], VSG control [22], and secondary control [3], [16] are not conductive to the flexible regulation of power and voltage of each phase, which could lead the TDG's phase with heavy load to be overloaded more easily, and cannot guarantee the voltage quality at all nodes to fulfill the requirements.

Manuscript received: May 1, 2020; revised: July 22, 2020; accepted: October 15, 2020. Date of CrossCheck: October 15, 2020. Date of online publication: November 26, 2020.

This work was supported in part by the National Natural Science Foundation of China (No. 51907098) and in part by the China Postdoctoral Science Foundation (No. 2020T130337).

J. Zhou, Y. Xu, and L. Yang are with the Tsinghua-Berkeley Shenzhen Institute (TBSI), Tsinghua Shenzhen International Graduate School (TsinghuaSIGS), Tsinghua University, Shenzhen 518055, China. (e-mail: jg_zhou@sz.tsinghua.edu.cn; xu.yinliang@sz.tsinghua.edu.cn; l-yang19@mails.tsinghua.edu.cn).

H. Sun (corresponding author) is with the Department of Electrical Engineering, State Key Laboratory of Power Systems, Tsinghua University, Beijing 100084, China (e-mail: shb@tsinghua.edu.cn).

DOI: 10.35833/MPCE.2020.000280

Obviously, MGs and IES are evolving into cyber-physical systems (CPSs) with the complex interaction with sophisticated software-based control and communication and physical networks, and with the development of energy internet [23]. Despite the advances of distributed approaches, their distributed nature could potentially make MGs vulnerable to malicious cyber-attacks and infiltration. The local measurements of sensors of DGs and the transmitted information between DG agents are likely to be attacked. These corrupted information could deteriorate the system performance and even cause instability via secondary controllers [24]. Currently, the bulk of existing research has been focused on attack detection in power systems [25] - [29]. For example, O. A. Beg *et al.* [25], [26] utilized a signal temporal logic method for attack detection in a DC MG. Sahoo *et al.* [27], [28] proposed a cooperative vulnerability factor based approach and a discordant element approach to detect the stealth attack in DC MGs. In order to address the influence of cyber-attacks, various works have been reported, which can be generally divided into two categories: ① detect/identify then correct/isolate; ② design resilient protocols directly. Regarding the first group of techniques, in [30], a Kullback-Liebler (KL) divergence-based mechanism was firstly developed to detect the attacks, and then a mitigation technique was proposed by utilizing the KL divergence factors to determine trust values that indicate the trustworthiness of the received neighboring information. In [31], an aperiodically intermittent strategy based on a random switching frequency was developed to realize the detection and isolation of corrupted communication links and controllers. However, this type of method usually has strict restrictions on the number of corrupted agents. If the number of the corrupted sensors exceeds the limits, it is impractical to securely detect and estimate the system states [32]. Moreover, some kinds of malicious attacks could bypass the existing detection methods to compromise the system performance [33]. Therefore, more research works focus on the second group of techniques. For example, Abhinav *et al.* [34], [35] proposed a confidence/trust-based control protocol for frequency and voltage control in networked AC MGs. More recently, distributed resilient control approaches have also been developed for energy storage system control [36] and thermostatically controlled load control [37]. Unlike most of the above research works, Zuo *et al.* [38] proposed a distributed resilient control approach where unbounded cyber-attacks were considered in MGs. In [39], a novel two-stage distributionally robust optimization was proposed to mitigate the risk of cyber-attacks in integration of electricity and gas systems. However, to the best of the authors' knowledge, cyber-attacks on the S/T-MGs have been neither systematically investigated nor addressed in a resilient distributed fashion.

With these motivations mentioned above, we focus on the S/T-MGs, where TDGs, SDGs and unbalanced loads are considered, as well as the adversarial cyber-attackers. An observer-based resilient distributed containment control approach will be developed for the coordination between SDGs and TDGs to achieve proper power sharing and voltage regulation. The concept of containment control has been discussed in [40] - [42]. The main contributions of this paper can be summarized as follows.

1) Load sharing and voltage regulation are investigated in islanded S/T-MGs, where TDGS, SDGs, and unbalanced loads are considered, as well as energy storage systems (ESSs). This is in contrast to many existing works which mainly focus on unbalanced loads and ideal direct current (DC) sources. The coordination between SDGs and TDGs is not adequately explored.

2) A resilient distributed containment control approach based on the idea of adaptive compensation is proposed for the S/T-MGs in the presence of different types of attacks on the communication links among DGs and/or leaders, on the relative information exchanged among DGs, and on the local measurements of DGs. Unlike some existing research works [3], [16], [22], the proposed approach along with the phase-independent virtual synchronous generator (P-VSG) approach allows for containment synchronization of power sharing and voltage regulation, and independent and flexible control of each phase of DGs, resulting in more reliable operation.

The remainder of this paper is structured as follows. The notations, preliminaries, modeling of the S/T-MGs and cyber-attacks, and problem formulation are presented in Section II. Section III discusses the proposed resilient distributed control strategy. Simulation results are provided to validate the proposed approach in Section IV. Conclusions are finally drawn in Section V.

II. Preliminaries, Modeling of S/T-MGs and Attacks, and Problem Formulation

A. Preliminaries

Notations: $P_Y(\boldsymbol{x})$ represents a projection of a vector $\boldsymbol{x}$ onto a closed convex set Y, i.e., $P_Y(\boldsymbol{x})=\arg\min_{\boldsymbol{y}\in Y}\|\boldsymbol{x}-\boldsymbol{y}\|$. $\boldsymbol{I}$ is the identity matrix, and $\boldsymbol{O}$ is the zero matrix. The sets of the leaders and the followers are denoted by $\mathcal{L}$ and $\mathcal{F}$, respectively.

Graph theory: many literatures have provided this knowledge. Please refer to [3], [42] due to page limits.

B. Modeling of S/T-MGs

Figure 1 depicts a possible S/T-MG consisting of SDGs, TDGs, and single-phase and three-phase loads. The source of DGs can be photovoltaic (PV), wind, hybrid PV/battery, or hybrid wind/battery. The SDGs are connected to the PCC through single-phase full-bridge inverters with *LC* filters, while three-phase four-wire inverters are adopted for TDGs. This type of MGs is typically unbalanced, which means that not only the load but also the DGs are unbalanced. In this scenario, the output power of each phase of TDGs can be different from each other, which, in turn, affects the MG loadability and reliability. All the DGs should cooperate with each other to provide reliable power supply and guarantee proper load sharing, admissible voltages, and ESS constraints.

To achieve flexible power sharing and voltage control and reliable operation for the S/T-MG, a P-VSG control approach proposed in [43] is adopted for the primary control in this paper, which is given by:

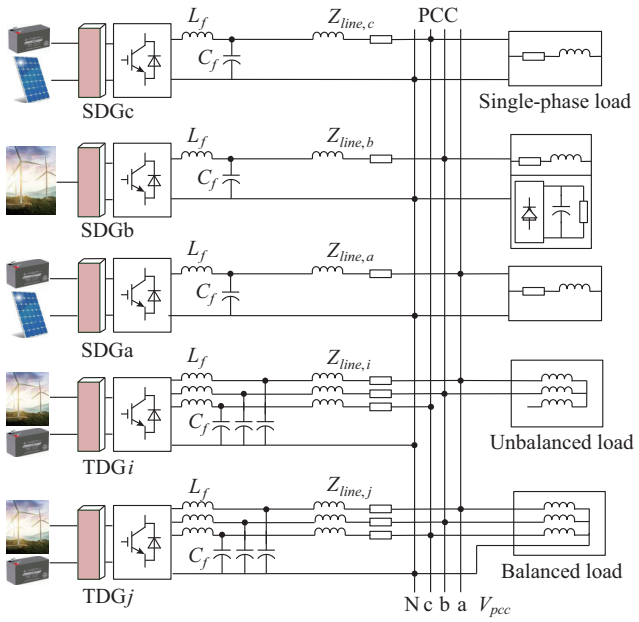

Fig. 1. A possible layout of an S/T-MG considered in this paper.

$$\dot{\theta}_i^{\#} = \omega_i^{\#} = \omega^* + \sum_{\flat=a,b,c} \Delta\omega_{i,\flat}^{\#} \tag{1}$$

$$M_i \Delta\dot{\omega}_{i,\flat}^{\#} = P_{res,i,\flat}^{\#} + P_{ess,i,\flat}^{\#} - P_{i,\flat}^{\#} - D_{p,i}\Delta\omega_{i,\flat}^{\#} \tag{2}$$

$$K_i \dot{E}_{i,\flat}^{\#} = Q_{set,i,\flat}^{\#} + \Delta Q_{i,\flat}^{\#} - Q_{i,\flat}^{\#} - D_{q,i}\left(E_{i,\flat}^{\#} - E^* - \Delta E_{i,\flat}^{\#}\right) \tag{3}$$

where $\dot{\theta}_i^{\#}$, $\omega_i^{\#}$, and $E_{i,\flat}^{\#}$ are the output power angle, angular frequency, and phase voltage magnitude of the DGs, respectively; ω^* and E^* are the desired angular frequency and voltage magnitude of the DGs, respectively; $P_{i,\flat}^{\#}$ and $Q_{i,\flat}^{\#}$ are the output active and reactive power of each phase, respectively; $P_{res,i,\flat}^{\#}$ and $P_{ess,i,\flat}^{\#}$ are the output power of RES and ESS used for phase $\flat$, respectively; $Q_{set,i,\flat}^{\#}$ is the reactive power set point of phase $\flat$; $\Delta Q_{i,\flat}^{\#}$ and $\Delta E_{i,\flat}^{\#}$ are the regulation terms of the reactive power and voltage magnitude of phase $\flat$, respectively, which will be determined by the secondary controllers; M_i and $D_{p,i}$ are the virtual inertia and damping constants, respectively; K_i and $D_{q,i}$ are the integrator gain to regulate the field excitation and the voltage droop coefficient, respectively; the superscript $\#=3ph$ or $1ph$ represents TDGs or SDGs, respectively; the subscript i represents the i^{th} DG; and $\flat=a,b,c$ represents phase a, phase b, and phase c, respectively.

Note that for SDG units, there is no sum of frequency deviations, and (1) can be rewritten as:

$$\dot{\theta}_{i,\flat}^{SDG} = \omega_{i,\flat}^{SDG} = \omega^* + \Delta\omega_{i,\flat}^{SDG} \quad \flat=a,b,c \tag{4}$$

where the superscript SDG represents the SDG units.

Then, from (1)-(3), the reference voltage of TDG units, $\boldsymbol{e}_i^{TDG} = \left[\, e_{i,a}^{TDG} \;\; e_{i,b}^{TDG} \;\; e_{i,c}^{TDG} \,\right]^{\mathrm{T}}$, can be generated by:

$$\boldsymbol{e}_i^{TDG} = \begin{bmatrix} E_{i,a}^{TDG} \sin\left[\left(\omega^* + \sum\Delta\omega_{i,\flat}^{TDG}\right)t\right] \\ E_{i,b}^{TDG} \sin\left[\left(\omega^* + \sum\Delta\omega_{i,\flat}^{TDG}\right)t - \dfrac{2\pi}{3}\right] \\ E_{i,c}^{TDG} \sin\left[\left(\omega^* + \sum\Delta\omega_{i,\flat}^{TDG}\right)t + \dfrac{2\pi}{3}\right] \end{bmatrix} \tag{5}$$

where $E_{i,\flat}^{TDG}$ ($\flat=a,b,c$) is the voltage amplitude of SDG units connected to phase $\flat$. The voltage $\boldsymbol{e}_{i,\flat}^{SDG}$ is given by:

$$\boldsymbol{e}_{i,\flat}^{SDG} = E_{i,\flat}^{SDG} \sin\left[\left(\omega^* + \Delta\omega_{i,\flat}^{SDG}\right)t + \varphi_\flat\right] \tag{6}$$

where $\varphi_\flat$ is set to be 0, $-\dfrac{2\pi}{3}$, and $\dfrac{2\pi}{3}$ for SDGs in phase a, phase b, and phase c, respectively.

Considering the faster dynamics of the *LC* filter, *RL* output connector, and voltage and current control loops of the DG units, and with the help of virtual impedance implemented in inner controllers, the dynamics from the reference voltage (5) to the active and reactive power delivered by the DG unit can be simply approximated as a first-order lag, i.e.,

$$\dot{P}_{i,\flat}^{\#} = -\tau^{-1}P_{i,\flat}^{\#} + \tau^{-1}P_{i,\flat,\max}^{\#}\left(\theta_i - \theta_g\right) \tag{7}$$

$$\dot{Q}_{i,\flat}^{\#} = -\tau^{-1}Q_{i,\flat}^{\#} + \tau^{-1}Q_{i,\flat,\max}^{\#}\left(E_{i,\flat}^{\#} - V_g\right) \tag{8}$$

where τ is the equivalent time constant; $P_{i,\flat,\max}^{\#}$ and $Q_{i,\flat,\max}^{\#}$ are the maximum active and reactive power of each phase that can be delivered by the DG unit, respectively; θ_i is the output voltage phase angle; θ_g is the voltage phase angle at PCC; and V_g is the voltage at PCC.

Define the following variables:

$$\begin{cases} \dot{P}_{ess,i,\flat}^{\#} = u_{i,\flat}^{\#,P} \\ \Delta\dot{Q}_{i,\flat}^{\#} = u_{i,\flat}^{\#,Q} \\ \Delta\dot{E}_{i,\flat}^{\#} = u_{i,\flat}^{\#,E} \end{cases} \tag{9}$$

where $u_{i,\flat}^{\#,P}$, $u_{i,\flat}^{\#,Q}$, and $u_{i,\flat}^{\#,E}$ are the control inputs of active power, reactive power, and voltage, respectively.

Define the state variable $\boldsymbol{x}_i(t) = \left(\boldsymbol{x}_{1i}^{\mathrm{T}}(t), \boldsymbol{v}_i^{\mathrm{T}}(t)\right)^{\mathrm{T}}$, $\boldsymbol{x}_{1i}(t) = \left(k_{i,p,\flat}^{\#}P_{i,\flat}^{\#}, \theta_i, \Delta\omega_{i,\flat}^{\#}, k_{i,q,\flat}^{\#}Q_{i,\flat}^{\#}, E_{i,\flat}^{\#}\right)^{\mathrm{T}}$, $\boldsymbol{v}_i(t) = \left(P_{ess,i,\flat}^{\#}, \Delta Q_{i,\flat}^{\#}, \Delta E_{i,\flat}^{\#}\right)^{\mathrm{T}}$, control input $\boldsymbol{u}_i(t) = \left(u_{i,\flat}^{\#,P}, u_{i,\flat}^{\#,Q}, u_{i,\flat}^{\#,E}\right)^{\mathrm{T}}$, and disturbance $\boldsymbol{d}_i(t) = \left(\theta_g, \sum_{\dagger}\Delta\omega_\dagger + \omega^*, P_{res,i,\flat}^{\#}, V_g, Q_{set,i,\flat}^{\#}, E^*\right)^{\mathrm{T}}$, $\dagger\neq\flat$, and $k_{i,p,\flat}^{\#}$ is the coefficient of active power sharing.

Then, by combining (1)-(3) and (7)-(9), we obtain:

$$\dot{\boldsymbol{x}}_i(t) = \boldsymbol{A}_i\boldsymbol{x}_i(t) + \boldsymbol{B}_i\boldsymbol{u}_i(t) + \boldsymbol{D}_i\boldsymbol{d}_i(t) \tag{10}$$

$$\boldsymbol{y}_i(t) = \boldsymbol{C}_i\boldsymbol{x}_i(t) \tag{11}$$

where $\boldsymbol{y}_i(t)$ is the output variable; $\boldsymbol{A}_i$, $\boldsymbol{B}_i$, $\boldsymbol{C}_i$, and $\boldsymbol{D}_i$ are defined in Appendix A.

It should be pointed out that in the real applications, by keeping accurate power sharing among DGs in the S/T-MGs, it is likely to result in deteriorated operation reliability, security and power quality since the three-phase output power and voltage can be seriously unbalanced, and some phases of the TDGs could be overloaded. Therefore, the reliability and security of the system can be improved by comprising the power sharing performance. And the output phase power of each TDG unit, voltages, and charging and discharging power should be controlled and kept within the permitted ranges, i.e.,

$$0 \le k_{i,p,\flat}^{\#}P_{i,\flat}^{\#} \le k_{i,p,\flat}^{\#}P_{i,\flat}^{\#,\max} \tag{12}$$

$$0 \le k_{i,q,\flat}^{\#}Q_{i,\flat}^{\#} \le k_{i,q,\flat}^{\#}Q_{i,\flat}^{\#,\max} \tag{13}$$

$$E_{ref}^{D} \le E_{i,\flat}^{\#}(t) \le E_{ref}^{U} \tag{14}$$

$$-P_{ess,i}^{\#,ch,\max} \le P_{ess,i}^{\#} \le P_{ess,i}^{\#,dch,\max} \tag{15}$$

where $P_{i,\flat}^{\#,\max}$ and $Q_{i,\flat}^{\#,\max}$ are the maximum output active and reactive power of phase $\flat$ of DG i, respectively; E_{ref}^{U} and E_{ref}^{D} are the maximum and minimum permitted voltage regulation requirements, respectively [44]; and $P_{ess,i}^{\#}$, $P_{ess,i}^{\#,ch,\max}$, and $P_{ess,i}^{\#,dch,\max}$ are the power and the permitted maximum charging and discharging values of ESSs, respectively.

Remark 1: the P-VSG control allows for independent and flexible power and voltage control for each phase of DGs, which is in contrast to conventional VSG [22]. Therefore, besides power sharing control, the voltage magnitude of each phase can also be independently controlled by regulating $E_i^{\#,*}$, thereby flexibly controlling the output voltage waveform if necessary for power quality improvement. Additionally, uncertain disturbances from renewable energy sources and constraints of ESSs are included in the established heterogeneous dynamics, which is different from many existing literatures where the disturbance and constraints are not considered. For TDGs, the sum of the frequency deviations among phases can accurately guarantee balanced phase shifts of 2π/3, and therefore, the phase shift balancing strategy can be avoided.

Assumption 1: in the constraints for ESSs, only the charging/discharging power is considered. We assume that the capacity of ESSs is sufficient in S/T-MGs system. Therefore, the constraint of state (SoC) of charge of ESSs is not included.

C. Modeling of Cyber-attacks

In this paper, cyber-attacks on local measurements of DG units, leaders and transmitted information between neighboring DG units are considered. With these attacks, the corrupted local measurements can be described as:

$$\begin{aligned}\underbrace{\left[k_{i,p,\flat}^{\#}\overline{P}_{i,\flat}^{\#}(t), k_{i,q,\flat}^{\#}\overline{Q}_{i,\flat}^{\#}(t), \overline{E}_{i,\flat}^{\#}(t), \overline{P}_{ess,i,\flat}^{\#}(t)\right]^{\mathrm{T}}}_{\bar{\boldsymbol{y}}_i^{\mathrm{T}}(t)} = \\ \underbrace{\left[k_{i,p,\flat}^{\#}P_{i,\flat}^{\#}(t), k_{i,q,\flat}^{\#}Q_{i,\flat}^{\#}(t), E_{i,\flat}^{\#}(t), P_{ess,i,\flat}^{\#}(t)\right]^{\mathrm{T}}}_{\boldsymbol{y}_i^{\mathrm{T}}(t)} + \\ \underbrace{\left[\phi_{p,i}^{a}(t), \phi_{q,i}^{a}(t), \phi_{e,i}^{a}(t), \phi_{ess,i}^{a}(t)\right]^{\mathrm{T}}}_{\left[\boldsymbol{\phi}_i^{a}(t)\right]^{\mathrm{T}}}\end{aligned} \tag{16}$$

where $\bar{\boldsymbol{y}}_i(t)$ is the corrupted output vector of the local measurements; and $\boldsymbol{\phi}_i^{a}(t)$ is the attack vector injected into the measurements by attackers. Similarly, the corrupted transmitted and leader information can be respectively described as:

$$\bar{\boldsymbol{y}}_{i,j}(t) = \boldsymbol{y}_j(t) + \boldsymbol{\phi}_{i,j}^{a}(t) \tag{17}$$

$$\overline{E}_{i,\flat,ref}^{U}(t) = E_{ref}^{U}(t) + \phi_{i,\flat,ref}^{U,a}(t) \tag{18}$$

$$\overline{E}_{i,\flat,ref}^{D}(t) = E_{ref}^{D}(t) + \phi_{i,\flat,ref}^{D,a}(t) \tag{19}$$

$$\overline{P}_{i,\flat}^{\#,\max}(t) = P_{i,\flat}^{\#,\max}(t) + \phi_{p,i,\flat,ref}^{U,a}(t) \tag{20}$$

$$\overline{Q}_{i,\flat}^{\#,\max}(t) = Q_{i,\flat}^{\#,\max}(t) + \phi_{q,i,\flat,ref}^{U,a}(t) \tag{21}$$

where $\boldsymbol{\phi}_{i,j}^{a}(t)$ is the attack vector injected to the communication links between agent i and j by the attackers; $\phi_{i,\flat,ref}^{U,a}(t)$, $\phi_{i,\flat,ref}^{D,a}(t)$, $\phi_{p,i,\flat,ref}^{U,a}(t)$, and $\phi_{q,i,\flat,ref}^{U,a}(t)$ are the information of attacks injected to the communication links from leaders to the follower DGs; the subscript ref denotes reference; the superscripts U and D denote the upper bound and down bound, respectively; and the superscript a denotes the attacks.

Assumption 2: considering the practical physical limitation, we assume that the attack signal is sparse and an attacker cannot inject large attack signals arbitrarily.

D. Problem Formulation

Let $P_{\mathcal{L}}$, $Q_{\mathcal{L}}$, $E_{\mathcal{L}}$, and $P_{ess,\mathcal{L}}$ denote the bounds of phase active and reactive power, voltage, charging/discharding power and (SoC), respectively. Then, $\boldsymbol{\Omega}$ is defined as the convex hull spanned by these leaders (bounds). With the developed models of the S/T-MGs and cyber-attacks as well as the control objective and definition of $\boldsymbol{\Omega}$ discussed above, we give the definition of the problem as follows.

Definition 1: Consider the dynamics of the S/T-MGs modeled as (10) and (11), the cyber-attacks described in (16)-(21) and the assumptions 1 and 2, the problem of resilient containment synchronization of power sharing, voltage regulation and charging/discharging power of ESSs is to design distributed secondary control protocols $\boldsymbol{u}_i(t)$ such that:

$$\lim_{t\to+\infty}\left\|\boldsymbol{y}_i(t) - \boldsymbol{P}_{\boldsymbol{\Omega}}\left(\boldsymbol{y}_i(t)\right)\right\| = 0 \tag{22}$$

where $\boldsymbol{y}_i(t) = \left(k_{i,p,\flat}^{\#}P_{i,\flat}^{\#}, k_{i,q,\flat}^{\#}Q_{i,\flat}^{\#}, E_{i,\flat}^{\#}, P_{ess,i,\flat}^{\#}\right)^{\mathrm{T}}$.

III. Design and Implementation of Resilient Distributed Secondary Controller

To counteract the effect of the cyber-attacks, we present a fully distributed resilient control approach based on the idea of adaptive compensation in this section. The controller is designed as:

$$\boldsymbol{u}_i(t) = \boldsymbol{K}_i\hat{\boldsymbol{x}}_i(t) + \boldsymbol{H}_i\hat{\boldsymbol{z}}_i(t) - \boldsymbol{H}_i\hat{\boldsymbol{d}}_i(t) \tag{23}$$

where $\hat{\boldsymbol{d}}_i(t)$ is an adaptive compensational parameter used to mitigate the effects of cyber-attacks; $\boldsymbol{K}_i$ and $\boldsymbol{H}_i$ are the controller gains; and $\hat{\boldsymbol{x}}_i(t)$ and $\hat{\boldsymbol{z}}_i(t)$ are the estimations of the system dynamics and dynamic compensators, respectively, which are obtained from the following distributed observers:

$$\dot{\hat{\boldsymbol{x}}}_i(t) = \boldsymbol{A}_i\hat{\boldsymbol{x}}_i(t) + \boldsymbol{B}_i\boldsymbol{u}_i(t) + \boldsymbol{B}_i\boldsymbol{H}_i\left(\bar{\boldsymbol{z}}_i(t) - \hat{\boldsymbol{z}}_i(t)\right) \tag{24}$$

$$\dot{\hat{\boldsymbol{z}}}_i(t) = \boldsymbol{F}_i\hat{\boldsymbol{z}}_i(t) + \boldsymbol{G}_i\hat{\boldsymbol{e}}_{yi}(t) \tag{25}$$

$$\dot{\hat{\boldsymbol{e}}}_{yi}(t) = \sum_{j\in\mathcal{F}} a_{ij}\left(\hat{\boldsymbol{y}}_j(t) - \hat{\boldsymbol{y}}_i(t)\right) + \sum_{k\in\mathcal{L}} g_{ik}\left(\boldsymbol{y}_k^{ref}(t) - \hat{\boldsymbol{y}}_i(t)\right) \tag{26}$$

where $\boldsymbol{F}_i$ and $\boldsymbol{G}_i$ are the control parameters; and $\hat{\boldsymbol{y}}(t)$ is the observers' output.

Then, the adaptive parameter $\hat{\boldsymbol{d}}_i(t)$ is updated by:

$$\dot{\hat{\boldsymbol{d}}}_i(t) = \boldsymbol{F}_i\hat{\boldsymbol{d}}_i(t) - \boldsymbol{G}_i\boldsymbol{C}_i\hat{\boldsymbol{\delta}}_i(t) \tag{27}$$

$$\begin{aligned}\dot{\hat{\boldsymbol{\delta}}}_i(t) = &\left(\boldsymbol{A}_i + \boldsymbol{B}_i\boldsymbol{K}_i\right)\left(\hat{\boldsymbol{x}}_i(t) + \hat{\boldsymbol{\delta}}_i(t) - \bar{\boldsymbol{x}}_i(t)\right) + \\ &\boldsymbol{B}_i\boldsymbol{H}_i\left(\hat{\boldsymbol{z}}_i(t) + \hat{\boldsymbol{d}}_i(t) - \bar{\boldsymbol{z}}_i(t)\right)\end{aligned} \tag{28}$$

With the proposed observer-based resilient distributed

adaptive control approach, the resilient containment synchronization of power sharing, voltage regulation and charging/discharging power of ESSs in the S/T-MGs can be realized, which is summarized as follows.

Theorem 1: consider the dynamics of the S/T-MGs modeled as (10) and (11) and assumptions 1 and 2. There exist matrices $\boldsymbol{P}_i$ and $\boldsymbol{L}_i$ such that the resilient containment synchronization of power sharing, voltage regulation and charging/discharging power of ESSs in the S/T-MGs under the cyber-attacks described in (16)-(21) can be solved by using the proposed distributed protocols (23)-(28) if the control parameters are designed as:

$$\begin{cases} \boldsymbol{H}_i = \boldsymbol{\Gamma}_i - \boldsymbol{K}_i \boldsymbol{\Pi}_i \\ \boldsymbol{F}_i = \boldsymbol{S} \\ \boldsymbol{K}_i \boldsymbol{\Phi}_i = -\dfrac{1}{\alpha_i} \boldsymbol{Q}_i^{-1} \left(\bar{\boldsymbol{B}}_i^{\mathrm{T}} \boldsymbol{P}_i + \boldsymbol{L}_i \right) \end{cases} \tag{29}$$

where $\boldsymbol{S}$ and $\boldsymbol{R}$ are the constructed leaders' state matrix and output matrix, respectively; α_i is a positive constant; $\boldsymbol{P}_i$ is a symmetric positive definite matrix; and $\boldsymbol{\Pi}_i$ and $\boldsymbol{\Gamma}_i$ can be obtained from the output regulator equations:

$$\begin{cases} \boldsymbol{A}_i \boldsymbol{\Pi}_i + \boldsymbol{B}_i \boldsymbol{\Gamma}_i = \boldsymbol{\Pi}_i \boldsymbol{S} \\ \boldsymbol{C}_i \boldsymbol{\Pi}_i = \boldsymbol{R} \end{cases} \tag{30}$$

$\boldsymbol{P}_i^{\mathrm{T}} = \boldsymbol{P}_i > \boldsymbol{0}$ is the solution to:

$$\boldsymbol{P}_i \bar{\boldsymbol{A}}_i + \bar{\boldsymbol{A}}_i^{\mathrm{T}} \boldsymbol{P}_i + \vec{\boldsymbol{C}}_i^{\mathrm{T}} \vec{\boldsymbol{C}}_i + \frac{1}{\gamma_i^2} \boldsymbol{P}_i \vec{\boldsymbol{G}}_i \vec{\boldsymbol{G}}_i^{\mathrm{T}} \boldsymbol{P}_i - \frac{1}{\alpha_i} \boldsymbol{P}_i \bar{\boldsymbol{B}}_i \boldsymbol{Q}_i^{-1} \bar{\boldsymbol{B}}_i^{\mathrm{T}} \boldsymbol{P}_i + \frac{1}{\alpha_i} \boldsymbol{L}_i^{\mathrm{T}} \boldsymbol{R}_i^{-1} \boldsymbol{L}_i = \boldsymbol{0} \tag{31}$$

where $\gamma_i < 1/\rho(\boldsymbol{\mathcal{A}})$, $\alpha_i > 0$, $\boldsymbol{\mathcal{A}} = [a_{ij}]$ is the adjacency matrix, and $\rho(\boldsymbol{\mathcal{A}})$ is the spectral radius of $\boldsymbol{\mathcal{A}}$. $\bar{\boldsymbol{A}}_i$, $\bar{\boldsymbol{B}}_i$, $\vec{\boldsymbol{C}}_i$ and $\vec{\boldsymbol{G}}_i$ are given in Appendix A.

Proof: please see Appendix A.

Figure 2 shows the control diagram of the proposed observer-based resilient distributed control approach, where where L_{fi} and C_{fi} are inductance and capacitance of LC filter, respectively. The upper right green box in the red box is used to generate the adaptive parameter $\hat{\boldsymbol{\delta}}_i$. Each DG agent utilizes its local and neighboring information to obtain the estimated information via the distributed observer, and then to update the controller $\boldsymbol{u}_i(t)$ and its corresponding adaptive compensation parameter $\hat{\boldsymbol{d}}_i(t)$. By doing this, the proposed control approach will be resilient to the cyber-attacks.

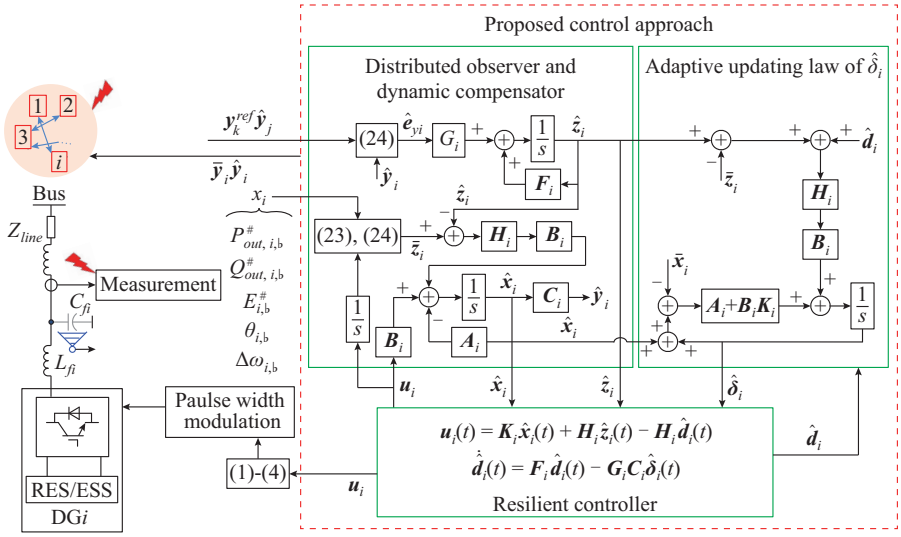

Fig. 2. Schematic control diagram of proposed resilient adaptive distributed control approach.

Remark 2: compared with the existing literature, salient features of the proposed distributed control can be summarized. ① Although the accuracy of power sharing among DG units may be compromised, the distributed containment controllers can guarantee that the output power of each phase is less than the maximum permitted value and that the unbalance of three-phase power of TDGs is improved. ② Containment voltage synchronization can be realized, i. e., the voltages of DG units can be regulated to admissible voltage profiles but not to the rated value, which is different from those in literature [3], [16]. ③ Distributed observers and adaptive compensation scheme can ensure uniformly ultimately bounded synchronization in the presence of cyber-attacks without the requirements of cyber-attack detection and isolation, and limitations on the number of corrupted agents.

Remark 3: The average active and reactive power of each phase of TDGs and as well as that of SDGs, which are utilized in the proposed distributed controller, can be calculated by:

$$P_{i,\flat}^{\#} = \frac{1}{2} E_{i,\flat}^{\#} I_{i,\flat}^{\#} \cos\psi \tag{32}$$

$$Q_{i,\flat}^{\#} = \frac{1}{2} E_{i,\flat}^{\#} I_{i,\flat}^{\#} \sin\psi \tag{33}$$

where $I_{i,\flat}^{\#}$ is the output current magnitude of the DGs; and ψ is the phase deviation between the voltage and current. These parameters can be obtained by using the Fourier analyser block in MATLAB/Simulink toolbox or the all-pass-filter-based phase-locked loop (PLL) systems [45]. Alternatively, the active and reactive power can also be calculated using other approaches and the details can be found in [43].

IV. Simulation Results

To validate the performance of the proposed control approach for the S/T-MG under various conditions, the S/T-MG depicted in Fig. 1 is simulated in MATLAB/Simulink environment, where two TDGs, three SDGs connected to phase a, phase b, and phase c, and unbalanced loads are considered. A single-phase H-bridge converter based three-phase four-wire DC/AC inverter with *LC* filters is adopted to interface the TDGs while a single-phase H-bridge inverter is used for the SDGs. The ratios of power ratings of DG units are considered as TDG1: TDG2: SDGa: SDGb: SDGc = 2:2:1:1:1. The parameters of the test MG system are listed in Table I. The cyber-attacks considered in the simulation are initiated at $t=1.5$ s, and at $t=2$ s, the loads in phase a and phase b are increased. Before $t=4$ s, the conventional distributed approach is implemented, and after that time, the proposed resilient distributed approach is activated to eliminate the effect of the cyber-attacks.

TABLE I
Parameters of MG Test System

Parameter	Symbol	Value	Unit
Nominal voltage	E^*	311	V
Nominal frequency	ω^*	$2\pi\times50$	rad
DC voltage	-	650 (TDGs)	V
	-	400 (SDGs)	V
DC capacitor	C_{dc}	2200	μF
Filter inductance	L_f	3	mH
Filter capacitor	C_f	15	μF
Power rating	$P_{i,\flat}^{TDG,\max}$	5	kW
	$P_a^{SDG,\max}$	7.5	kW
	$P_b^{SDG,\max}$	7.5	kW
	$P_c^{SDG,\max}$	7.5	kW
Line impedance	$Z_{line,i}$	0.07	Ω
	$Z_{line,a}$	0.07	Ω
	$Z_{line,b}$	0.07	Ω
	$Z_{line,c}$	0.07	Ω
Virtual inertia	M_i	0.04	kWs^2
Virtual damping	$D_{p,i}$	19.7	kW/Hz
Virtual gain	K_i	7.5	-
Droop coefficient	$2D_{q,i}$	6 or 3	kvar/V

The communication topology of agents is shown in Fig. 3 in detail, in which each phase of the DG units including TDGs and SDGs has a dedicated control agent. The TDG and SDG agents are represented by highlighted circle and square nodes, respectively. These TDG and SDG agents with the same phases are connected together, forming a ring-shape communication topology for data exchange. The TDG1 and TDG2 can receive the upper and lower reference information from leaders. Figure 3(a) shows the communication topology without cyber-attack. Besides, different scenarios of the cyber-attacks are considered during the simulation: ① attacks injected into the communication links from leaders to followers (Fig. 3(b)); ② attacks injected into communication links between neighboring DG agents (Fig. 3(c)); and ③ attacks injected into the local measurements of SDGs (Fig. 3(d)). The simulation is divided into five cases discussed in detail as follows.

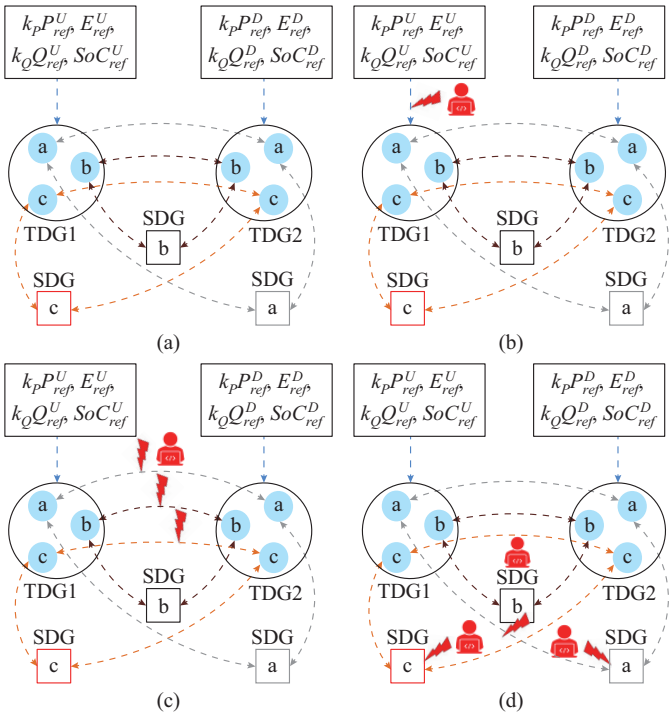

Fig. 3. Communication topology of agents for S/T-MG. (a) Communication topology without cyber-attack. (b) Attacks injected into the communication links from leaders to followers. (c) Attacks injected into communication links between neighboring DG agents. (d) Attacks injected into local measurements of SDGs.

A. Case 1: Attacks on Communication Links Between Leaders and Followers

In this case, the cyber-attacks on the communication link from the upper voltage reference leader to the TDG1 are considered and modeled as $\phi^{U,a}_{E,1,a,ref}(t)=-0.1t+10t\sin(6\pi t)+2$, $\phi^{U,a}_{E,1,b,ref}(t)=-0.1t+6t\sin(6\pi t)+3$, $\phi^{U,a}_{E,1,c,ref}(t)=-0.1t+8t\sin(6\pi t)-1$, where the subscript E represents the voltage. Figure 4 shows the performance comparison of conventional distributed cooperative control approach in [43] and the proposed observer-based resilient distributed adaptive control approach in this paper.

As shown in Fig. 4, the active and reactive power, voltages of the TDG1, TDG2, SDGa, SDGb and SDGc, and the charging/discharging power of ESSs are deteriorated due to the corrupted upper voltage reference information at $t=1.5$ s, when the conventional distributed approach is utilized. The voltage control performance is seriously affected, and it cannot be stably maintained. The voltages oscillate obviously. Because of the relationship between reactive power and voltage, the reactive power is also obviously affected, but the influence of the cyber-attack on active power is not obvious. After $t=4$ s, we activate the proposed resilient adaptive control approach. With the help of the distributed observer (24)-(26) and adaptive compensation parameter $\hat{\boldsymbol{d}}_i(t)$, the influ-

ence of the cyber-attacks on the upper reference voltage leader can be effectively mitigated. Therefore, the active and reactive power and DG voltages can be controlled to the expected values and ranges. But it could take a longer time to converge to the steady state. That is to say, the satisfied containment synchronization of the load power sharing and voltage regulation is asymptotically achieved.

B. Case 2: Attacks on Communication Links Between Neighboring DG Agents

As shown in Fig. 3(c), the cyber-attacks on the communication link between TDG1 and TDG2 is considered in the second case. The information received by TDG1 from its neighbor TDG2 is attacked at $t=1.5$ s, and the attack is modeled as $\phi^a_{p,1,2,j}(t) = -500t + 5000t\sin(6\pi t) + 2000 = \phi^a_{q,1,2,j}(t)$, where the subscripts p and q represent active and reactive power, respectively. Figure 5 shows the performances of conventional distributed cooperative control approach in [43] and the proposed observer-based resilient distributed adaptive control approach in this paper.

As shown in Fig. 5, in the presence of cyber-attack on the communication link between TDG1 and TDG2, the conventional cooperative controller utilized for TDG1 is misled. Then, the controllers of the other DG units are also indirectly influenced due to the connected communication topology and interaction between the physical MG layer and cyber layer. Therefore, the conventional cooperative controller fails to maintain the overall stability of the system. Moreover, although only the active and reactive power information is attacked, the voltages and charging/discharging power are also seriously affected, and their stability cannot be maintained. However, when the proposed resilient approach is activated at $t=4$ s, the load active and reactive power sharing, the magnitudes of the DG voltages as well as the charging/discharging power of ESSs, can be regulated and kept within the prescribed range. Thus, the resilient secondary voltage and load sharing containment synchronization problems are solved under cyber-attacks for the S/T-MGs.

C. Case 3: Attacks on Local Measurements of SDGs

Finally, in the last case, cyber-attacks injected into the local measurements of SDGa, SDGb, and SDGc are considered. Specifically, as shown in Fig. 3(d), we consider the scenario that the local measurements of output active and reactive powers of the SDG units are corrupted by some malicious attackers. These corrupted measurements are directly fed back to the local controllers to deteriorate the system control performance. The attacks are modeled as $\phi^a_{p,SDG,a}(t) = 5000t\sin(6\pi t) = \phi^a_{q,SDG,a}(t)$, $\phi^a_{p,SDG,b}(t) = \phi^a_{q,SDG,b}(t) = -500t$, $\phi^a_{p,SDG,c}(t) = \phi^a_{q,SDG,c}(t) = 2000$. Figure 6 shows the performances of conventional distributed cooperative control approach in [43] and the proposed observer-based resilient distributed adaptive control approach in this paper.

It can be observed from Fig. 6 that the local measurements of the active and reactive power of the SDG units are corrupted by the malicious attack signals, and then fed back into the their local controllers to mislead the control objects. Therefore, the expected active and reactive power sharing among DG units cannot be maintained by the conventional controllers. Moreover, the voltages of DG units are also seri-

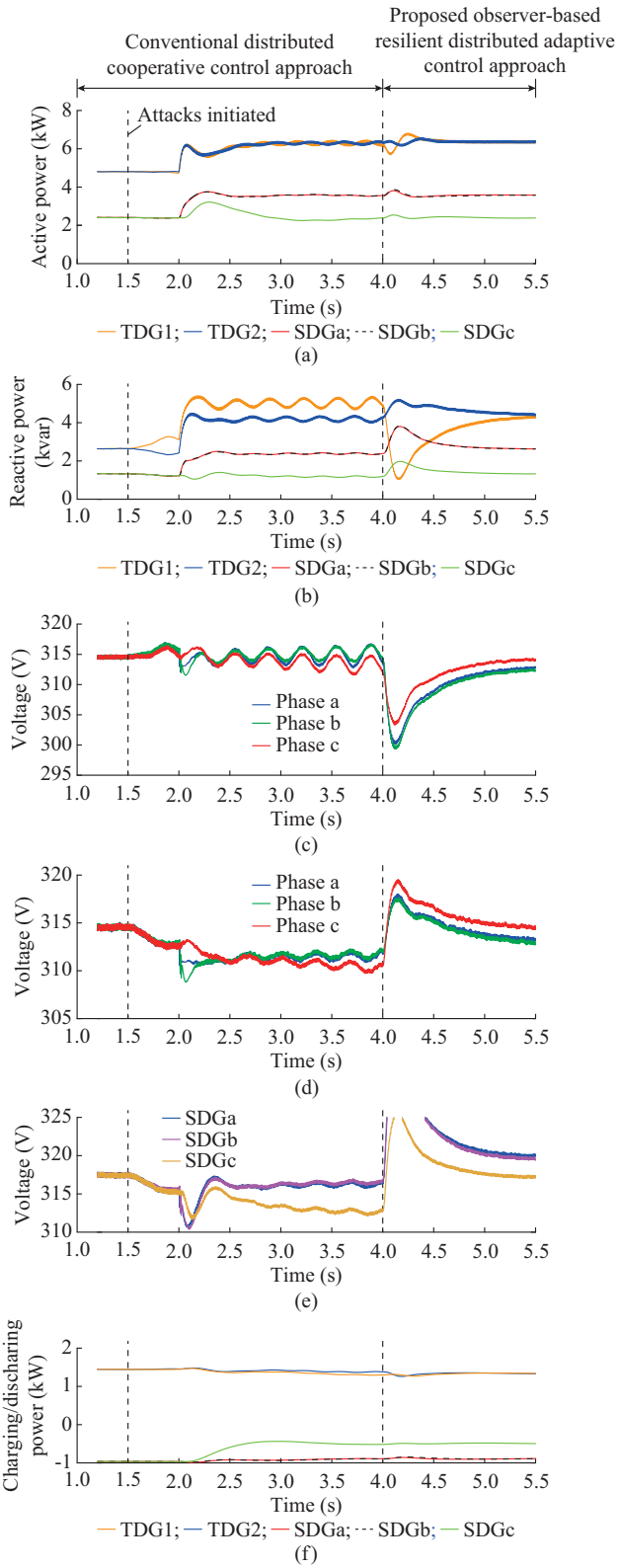

Fig. 4. Performance of conventional distributed cooperative control approach and proposed observer-based resilient distributed adaptive control approach in presence of cyber-attacks injected into communication links from leaders to followers. (a) Active power. (b) Reactive power. (c) Voltage of TDG1. (d) Voltage of TDG2. (e) Voltage of SDG. (f) Charging/discharging power.

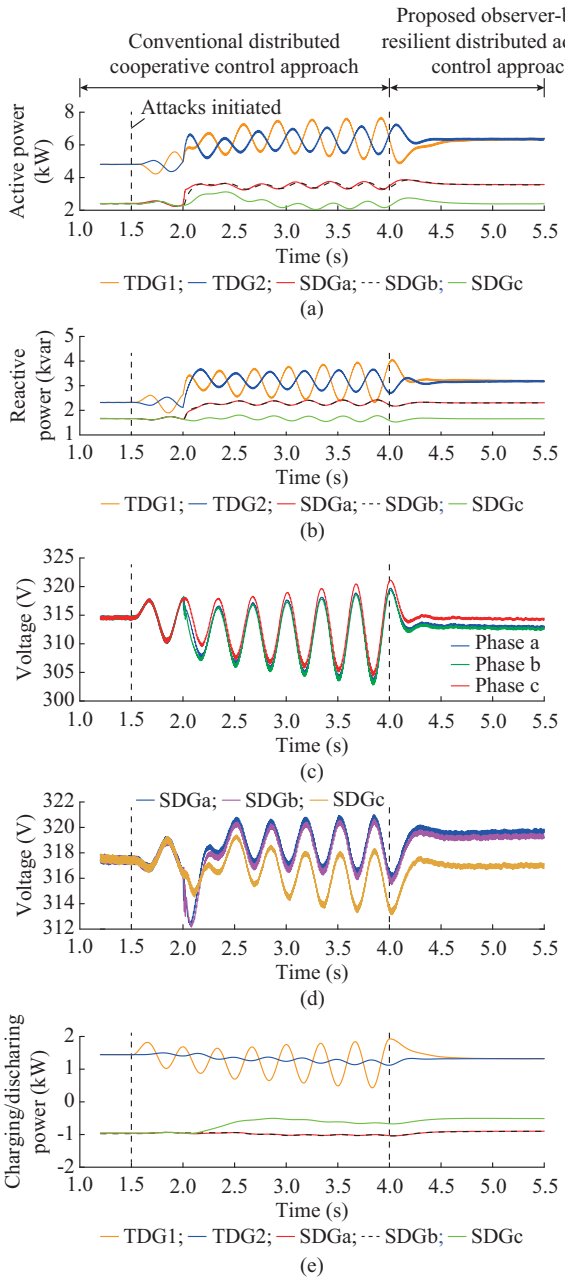

Fig. 5. Performance of conventional distributed cooperative control approach and proposed observer-based resilient distributed adaptive control approach in presence of cyber-attacks injected into communication links between neighboring DG agents. (a) Active power. (b) Reactive power. (c) Voltage of TDG1. (d) Voltage of SDG. (e) Charging/discharging power.

ously disrupted. The conventional cooperative controllers cannot maintain the voltage stability. Additionally, the charging/discharging power of ESSs are disrupted as well due to the misled active power sharing. After $t=4$ s, however, the containment synchronization of the active and reactive power sharing and voltage regulation is achieved again with the activation of the proposed resilient distributed adaptive control approach.

D. Case 4: Plug-and-play and Communication Time Delay

In this case, the plug-and-play and the communication time delay are considered. The condition is the same as that of Case 2 except the activation time of the proposed resilient distributed approach. In this case, from $t=3$ s, the proposed approach is activated. At $t=2.5$ s, SDGb is plugged out and then plugged in at $t=4$ s. Additionally, during the simulation, a communication time delay of 100 ms is also considered. Figure 7 shows the simulation results. It can be observed that the approach has good plug-and-play performance and that the active and reactive power can converge to the expected steady state under 100 ms time delay. This can meet the requirement of IEEE standard.

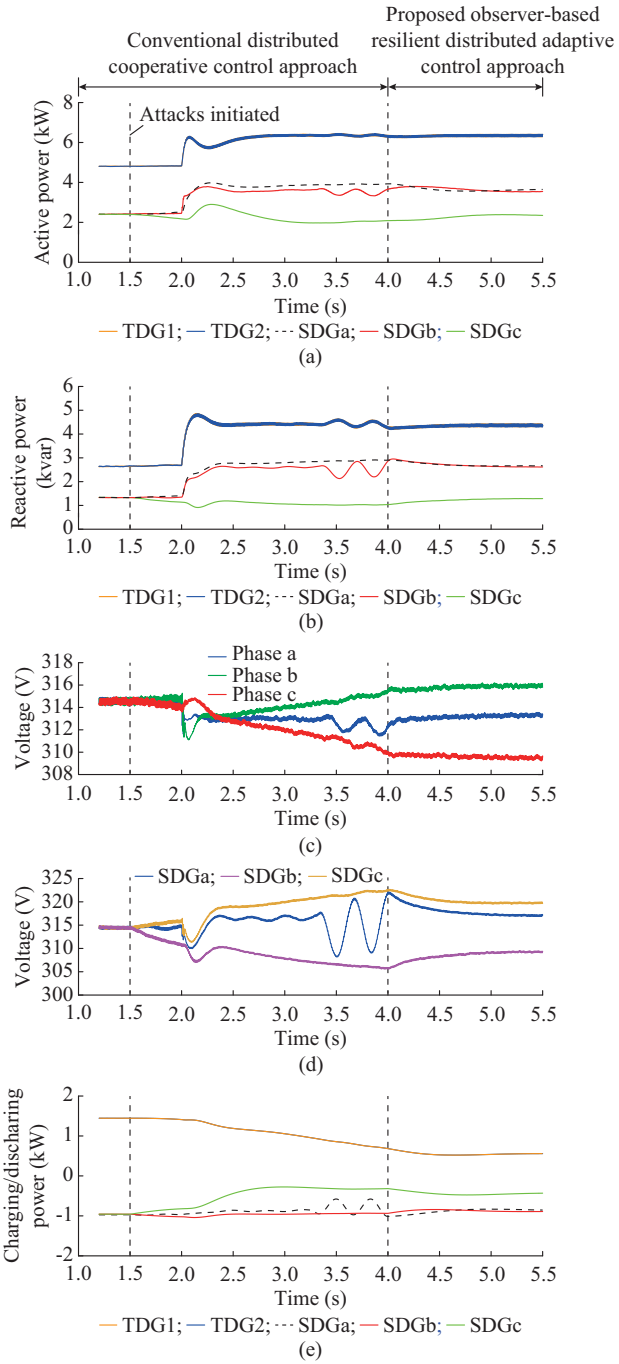

Fig. 6. Performance of conventional distributed cooperative control approach and proposed observer-based resilient distributed adaptive control approach in presence of cyber-attacks injected into local measurements of SDGs. (a) Active power. (b) Reactive power. (c) Voltage of TDG1. (d) Voltage of SDG. (e) Charging/discharging power.

E. Case 5: Comparison of Phase Shift Performance

In this case, we mainly validate the performance of the proposed P-VSG approach and compare it with the conventional VSG approach. Figure 8 shows the phase shifts and phase difference of three-phase converters, where PDab, PDbc, PDca are the phase differences between phases a and b, b and c, and c and a, respectively. It can be observed from Fig. 8 that an accurate phase shift of 120° of the output voltage of the three-phase converters is achieved with the conventional approach. The phase difference is almost zero. Also, the accurate phase shift of 120° of the output voltage of the three-phase converters is achieved with the proposed P-VSG approach, which is even better than that of the conventional approach. The maximum phase difference at steady state is about 0.00142 (0.17°), which is reduced by approximately 34.6% compared with that of the conventional VSG approach (about 0.00215 (0.26°)). This validates the effectiveness of the proposed approach.

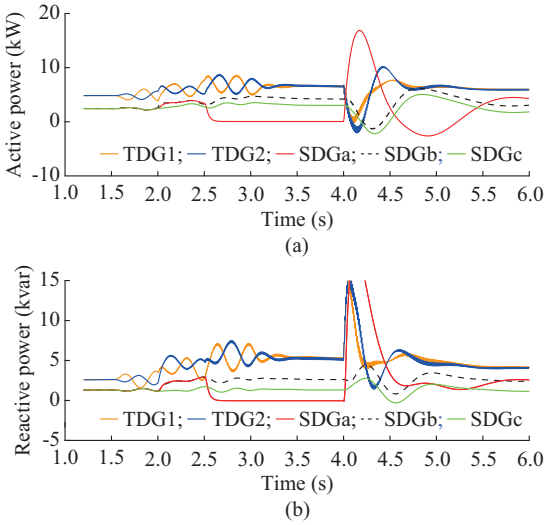

Fig. 7. Simulation results considering plug-and-play and communication delay of 100 ms. (a) Active power of DGs. (b) Reactive power of DGs.

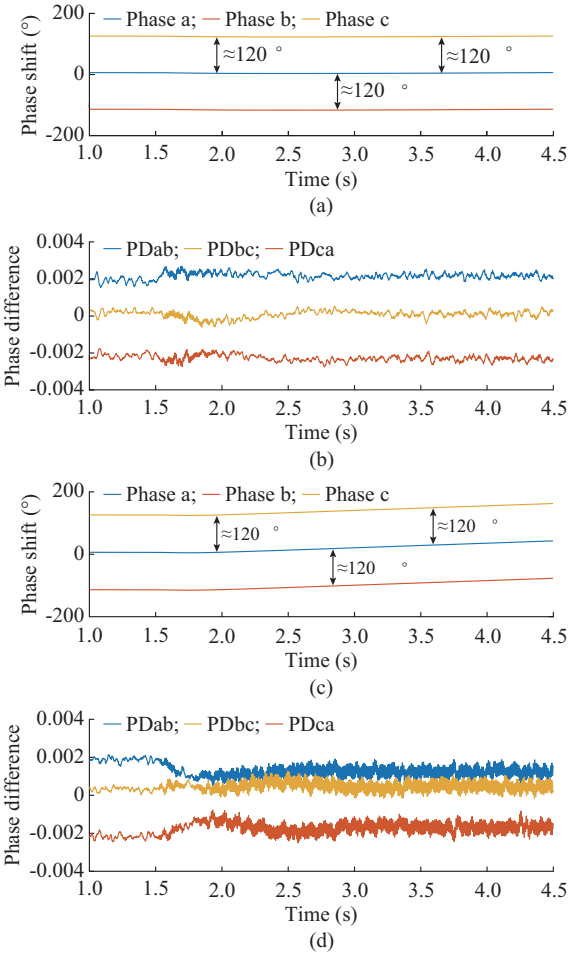

Fig. 8. Phase shifts and phase difference of three-phase converters. (a) Phase shifts of conventional approach. (b) Phase differences of conventional approach. (c) Phase shifts of proposed approach. (d) Phase differences of proposed approach.

V. Conclusion

We have considered a novel type of MGs, i.e., S/T-MGs, with the integration of TDGs, SDGs, unbalanced loads, and ESSs in this paper. Also, cyber-attacks on local measurements of DGs, leader references, and information transmitted between DG agents are considered when designing the controller. To achieve the flexible and reliable operation and control of DGs in the S/T-MGs, and to guarantee satisfactory power sharing and voltage control performance, the problem is formulated as a distributed output containment control problem based on the established heterogeneous dynamics of DG units. Then, an attack-resilient distributed control based on the idea of adaptive compensation is developed by designing a distributed adaptive observer. With this approach, the effect of the cyber-attacks can be neutralized to ensure the stability of the system and preserve the containment power sharing and voltage synchronization. Finally, several simulation results verify the effectiveness of the proposed approach.

However, the containment power sharing and voltage synchronization do not mean that power quality such as voltage unbalance factors in the S/T-MGs can satisfy the standard. Therefore, the future work will focus on the resilient distributed control design for the improvement of power quality in S/T-MGs. Another interesting direction is how to further explore the coordination among TDGs, SDGs, ESSs and flexible loads.

Appendix A

A. Parameters in Section II-B

The parameters in Section II-B include: $\mathring{\boldsymbol{A}}_i = \begin{bmatrix} \tilde{\boldsymbol{A}}_{i,1} & \boldsymbol{O} \\ \boldsymbol{O} & \tilde{\boldsymbol{A}}_{i,2} \end{bmatrix}$, $\mathring{\boldsymbol{C}}_i = \begin{bmatrix} \tilde{\boldsymbol{C}}_{i,1} & \tilde{\boldsymbol{C}}_{i,2} \end{bmatrix}$, $\tilde{\boldsymbol{C}}_{i,1} = [1 \ 0 \ 0]$, $\tilde{\boldsymbol{C}}_{i,2} = [1 \ 1]$, $\mathring{\boldsymbol{B}}_i = \begin{bmatrix} \tilde{\boldsymbol{B}}_{i,1} \\ \tilde{\boldsymbol{B}}_{i,2} \end{bmatrix}$, $\mathring{\boldsymbol{D}}_i = \begin{bmatrix} \tilde{\boldsymbol{D}}_{i,1} & \boldsymbol{O} \\ \boldsymbol{O} & \tilde{\boldsymbol{D}}_{i,2} \end{bmatrix}$,

$$\tilde{\boldsymbol{A}}_{i,1} = \begin{bmatrix} -\frac{1}{\tau} & -\frac{k^{\#}_{i,p,k} P^{\#}_{i,\flat,\max}}{\tau} & 0 \\ 0 & 0 & 1 \\ -\frac{1}{M_i k^{\#}_{i,p,\flat}} & 0 & -\frac{D_{p,i}}{M_i} \end{bmatrix}, \quad \tilde{\boldsymbol{A}}_{i,2} = \begin{bmatrix} -\frac{1}{\tau} & -\frac{k^{\#}_{i,q,j} Q^{\#}_{i,\flat,\max}}{\tau} \\ -K_i^{-1} k^{\#,-1}_{i,q,\flat} & -D_{q,i} K_i^{-1} \end{bmatrix},$$

$$\tilde{\boldsymbol{B}}_{i,1} = \begin{bmatrix} 0 & 0 & 0 \\ 0 & 0 & 0 \\ M_i^{-1} & 0 & 0 \end{bmatrix}, \quad \tilde{\boldsymbol{B}}_{i,2} =$$

$$\begin{bmatrix} 0 & 0 & 0 \\ 0 & K_i^{-1} & \dfrac{D_{q,i}}{K_i} \end{bmatrix},\quad \tilde{\boldsymbol{D}}_{i,1}=\begin{bmatrix} -\dfrac{k_{i,p,\mathrm{b}}^{\#}P_{i,\mathrm{b},\max}^{\#}}{\tau} & 0 & 0 \\ 0 & 1 & 0 \\ 0 & 0 & M_i^{-1} \end{bmatrix},\quad \boldsymbol{B}_i=\begin{bmatrix} \boldsymbol{O} \\ \boldsymbol{I}_i \end{bmatrix},$$

$$\tilde{\boldsymbol{D}}_{i,2}=\begin{bmatrix} -\dfrac{k_{i,q,\mathrm{b}}^{\#}Q_{i,\mathrm{b},\max}^{\#}}{\tau} & 0 & 0 \\ 0 & K_i^{-1} & \dfrac{D_{q,i}}{K_i} \end{bmatrix},\ \boldsymbol{D}_i=\begin{bmatrix} \mathring{\boldsymbol{D}}_i \\ \boldsymbol{O} \end{bmatrix},\ \boldsymbol{A}_i=\begin{bmatrix} \mathring{\boldsymbol{A}}_i & \mathring{\boldsymbol{B}}_i \\ \boldsymbol{O} & \boldsymbol{O} \end{bmatrix},\ \text{and}$$

$$\boldsymbol{C}_i=\begin{bmatrix} \mathring{\boldsymbol{C}}_i & 1 & 0 \end{bmatrix}.$$

B. Proof of Theorem 1

The proof is divided into two steps.

Step 1: prove the containment convergence of the observer's output $\hat{\boldsymbol{y}}_i(t)$ to the dynamic convex hull spanned by the leaders' outputs.

Step 2: prove the containment convergence of each DG's output $\boldsymbol{y}_i(t)$ to the estimation observer's output $\hat{\boldsymbol{y}}_i(t)$.

The process of the proof of *Steps 1* and *2* is motivated by [42]. For more details of interest, please refer to [42]. This ends the proof.

C. Parameters in Section III

The parameters in Section III are given as: $\bar{\boldsymbol{A}}_i=\begin{bmatrix} \boldsymbol{A}_i & \boldsymbol{B}_i\boldsymbol{\Gamma}_i \\ -\boldsymbol{G}_i\boldsymbol{C}_i & \boldsymbol{S} \end{bmatrix}$, $\bar{\boldsymbol{B}}_i=\begin{bmatrix} \boldsymbol{B}_i \\ \boldsymbol{O} \end{bmatrix}$, $\vec{\boldsymbol{C}}_i=[\boldsymbol{C}_i \quad \boldsymbol{O}]$, and $\vec{\boldsymbol{G}}_i=[\boldsymbol{O} \quad \boldsymbol{G}_i^{\mathrm{T}}]^{\mathrm{T}}$.

REFERENCES

[1] J. M. Guerrero, M. Chandorkar, T.-L. Lee *et al*., "Advanced control architectures for intelligent microgrids–part I: decentralized and hierarchical control," *IEEE Transactions on Industrial Electronics*, vol. 60, no. 4, pp. 1254-1262, Apr. 2013.

[2] J. Zhou, Y. Xu, H. Sun *et al*., "Distributed event-triggered H_∞ consensus based current sharing control of DC microgrids considering uncertainties," *IEEE Transactions on Industrial Informatics*, vol. 16, no. 12, pp. 7413-7425, Dec. 2020.

[3] J. Zhou, S. Kim, H. Zhang *et al*., "Consensus-based distributed control for accurate reactive, harmonic and imbalance power sharing in microgrids," *IEEE Transactions on Smart Grid*, vol. 9, no. 4, pp. 2453-2467, Jul. 2018.

[4] A. Hintz, U. R. Prasanna, and K. Rajashekara, "Comparative study of the three-phase grid-connected inverter sharing unbalanced three-phase and/or single-phase systems," *IEEE Transactions on Industrial Applications*, vol. 52, no. 6, pp. 5156-5164, Nov. 2016.

[5] E. Espina, R. Cárdenas-Dobson, M. Espinoza *et al*., "Cooperative regulation of imbalances in three-phase four-wire microgrids using single-phase droop control and secondary control algorithms," *IEEE Transactions on Power Electronics*, vol. 35, no. 2, pp. 1978-1992, Feb. 2020.

[6] Q. Sun, J. Zhou, J. M. Guerrero *et al*., "Hybrid three-phase/single-phase microgrid architecture with power management capabilities," *IEEE Transactions on Power Electronics*, vol. 30, no. 10, pp. 5964-5977, Oct. 2015.

[7] S. A. Raza and J. Jiang, "Intra- and inter-phase power management and control of a residential microgrid at the distribution level," *IEEE Transactions on Smart Grid*, vol. 10, no. 6, pp. 6839-6848, Nov. 2019.

[8] Y. Karimi, H. Oraee, and J. M. Guerrero, "Decentralized method for load sharing and power management in a hybrid single/three-phase-islanded microgrid consisting of hybrid source PV/battery units," *IEEE Transactions on Power Electronics*, vol. 32, no. 8, pp. 6135-6144, Aug. 2017.

[9] M. A. Allam, A. A. Said, M. Kazerani *et al*., "A novel dynamic power routing scheme to maximize loadability of islanded hybrid AC/DC microgrids under unbalanced AC loading," *IEEE Transactions on Smart Grid*, vol. 9, no. 6, pp. 5798-5809, Nov. 2018.

[10] Y. Li, H. Zhang, X. Liang *et al*., "Event-triggered-based distributed cooperative energy management for multienergy systems," *IEEE Transactions on Industrial Informatics*, vol. 15, no. 4, pp. 2008-2022, Apr. 2019.

[11] Y. Li, D. W. Gao, W. Gao *et al*., "Double-mode energy management for multi-energy system via distributed dynamic event-triggered newton-raphson algorithm," *IEEE Transactions on Smart Grid*, vol. 11, no. 6, pp. 5339-5356, Nov. 2020.

[12] Y. Li, H. Zhang, B. Huang *et al*., "A distributed Newton-Raphson-based coordination algorithm for multi-agent optimization with discrete-time communication," *Neural Computing and Applications*, vol. 32, no. 9, pp. 4649-4663, Oct. 2020.

[13] J. Zhou, Y. Xu, H. Sun *et al*., "Distributed power management for networked AC/DC microgrids with unbalanced microgrids," *IEEE Transactions on Industrial Informatics*, vol. 16, no. 3, pp. 1655-1667, Mar. 2020.

[14] L. Meng and J. M. Guerrero, "Optimization for customized power quality service in multibus microgrids," *IEEE Transactions on Industrial Electronics*, vol. 64, no. 11, pp. 8767-8777, Nov. 2017.

[15] M. M. Hashempour, T. Lee, M. Savaghebi *et al*., "Real-time supervisory control for power quality improvement of multi-area microgrids," *IEEE Systems Journal*, vol. 13, no. 1, pp. 864-874, Mar. 2019.

[16] L. Meng X. Zhao, F. Tang *et al*., "Distributed voltage unbalance compensation in islanded microgrids by using a dynamic consensus algorithm," *IEEE Transactions on Power Electronics*, vol. 31, no. 1, pp. 827-838, Jan. 2016.

[17] D. I. Brandao, T. Caldognetto, F. P. Marafão *et al*., "Centralized control of distributed single-phase inverters arbitrarily connected to three-phase four-wire microgrids," *IEEE Transactions on Smart Grid*, vol. 8, no. 1, pp. 437-446, Jan. 2017.

[18] F. Nejabatkhah and Y. W. Li, "Flexible unbalanced compensation of three-phase distribution system using single-phase distributed generation inverters," *IEEE Transactions on Smart Grid*, vol. 10, no. 2, pp. 1845-1857, Mar. 2019.

[19] A. Mortezaei, M. G. Simões, M. Savaghebi *et al*., "Cooperative control of multi-master-slave islanded microgrid with power quality enhancement based on conservative power theory," *IEEE Transactions on Smart Grid*, vol. 9, no. 4, pp. 2964-2975, Jul. 2018.

[20] C. Burgos-Mellado, J. J. Llanos, R. Cárdenas *et al.*, "Distributed control strategy based on a consensus algorithm and on the conservative power theory for imbalance and harmonic sharing in 4-wire microgrids," *IEEE Transactions on Smart Grid*, vol. 11, no. 2, pp. 1604-1619, Mar. 2020.

[21] D. I. Brandao, L. S. Araujo, A. M. S. Alonso *et al*., "Coordinated control of distributed three- and single-phase inverters connected to three-phase three-wire microgrids," *IEEE Journal of Emerging and Selected Topics in Power Electronics*, vol. 8, no. 4, pp. 3861-3877, Dec. 2020.

[22] Q. Zhong, "Virtual synchronous machines: a unified interface for grid integration," *IEEE Power Electronics Magazine*, vol. 3, no. 4, pp. 18-27, Dec. 2016.

[23] H. Zhang, Y. Li, and D. W. Gao *et al.*, "Distributed optimal energy management for energy internet," *IEEE Transactions on Industrial Informatics*, vol. 13, no. 6, pp. 3081-3097, Dec. 2017.

[24] X. Liu, M. Shahidehpour, Y. Cao *et al.*, "Microgrid risk analysis considering the impact of cyber-attacks on solar PV and ESS control systems," *IEEE Transactions on Smart Grid*, vol. 8, no. 3, pp. 1330-1339, May 2017.

[25] O. A. Beg, T. T. Johnson, and A. Davoudi, "Detection of false-data injection attacks in cyber-physical DC microgrids," *IEEE Transactions on Industrial Informatics*, vol. 13, no. 5, pp. 2693-2703, Oct. 2017.

[26] O. A. Beg, L. V. Nguyen, T. T. Johnson *et al.*, "Signal temporal logic-based attack detection in DC microgrids," *IEEE Transactions on Smart Grid*, vol. 10, no. 4, pp. 3585-3595, Jul. 2019.

[27] S. Sahoo, S. Mishra, J. C. Peng *et al.*, "A stealth cyber-attack detection strategy for DC microgrids," *IEEE Transactions on Power Electronics*, vol. 34, no. 8, pp. 8162-8174, Aug. 2019.

[28] S. Sahoo, J. C. Peng, A. Devakumar *et al.*, "On detection of false data in cooperative DC microgrids–a discordant element approach," *IEEE Transactions on Industrial Electronics*, vol. 67, no. 8, pp. 6562-6571, Aug. 2020.

[29] T. Huang, B. Satchidanandan, P. R. Kumar *et al.*, "An online detection framework for cyber-attacks on automatic generation control," *IEEE Transactions on Power Systems*, vol. 33, no. 6, pp. 6816-6827, Nov. 2018.

[30] A. Mustafa, B. Poudel, A. Bidram *et al.*, "Detection and mitigation of data manipulation attacks in AC microgrids," *IEEE Transactions on Smart Grid*, vol. 11, no. 3, pp. 2588-2603, May 2020.

[31] Q. Zhou, M. Shahidehpour, A. Alabdulwahab *et al.*, "A cyber-attack resilient distributed control strategy in islanded microgrids," *IEEE Transactions on Smart Grid*, vol. 11, no. 5, pp. 3690-3701, Sept. 2020.
[32] L. An and G. Yang, "Secure state estimation against sparse sensor attacks with adaptive switching mechanism," *IEEE Transactions on Automatic Control*, vol. 63, no. 8, pp. 2596-2603, Aug. 2018.
[33] F. Pasqualetti, F. Dorfler, and F. Bullo, "Attack detection and identification in cyber-physical systems," *IEEE Transactions on Automatic Control*, vol. 58, no. 11, pp. 2715-2729, Nov. 2013.
[34] S. Abhinav, H. Modares, F. L. Lewis *et al.*, "Synchrony in networked microgrids under attacks," *IEEE Transactions on Smart Grid*, vol. 9, no. 6, pp. 6731-6741, Nov. 2018.
[35] S. Abhinav, H. Modares, F. L. Lewis *et al.*, "Resilient cooperative control of DC microgrids," *IEEE Transactions on Smart Grid*, vol. 10, no. 1, pp. 1083-1085, Jan. 2019.
[36] C. Deng, Y. Wang, C. Wen *et al.*, "Distributed resilient control for energy storage systems in cyber-physical microgrids," *IEEE Transactions on Industrial Informatics*, vol. 17, no. 2, pp. 1331-1341, Feb. 2021.
[37] Y. Wan, C. Long, R. Deng *et al.*, "Distributed event-based control for thermostatically controlled loads under hybrid cyber-attacks," *IEEE Transactions on Cybernetics*, vol. 51, no. 11, pp. 5314-5327, Nov. 2021.
[38] S. Zuo, O. A. Beg, F. L. Lewis *et al.*, "Resilient networked AC microgrids under unbounded cyber-attacks," *IEEE Transactions on Smart Grid*, vol. 11, no. 5, pp. 3785-3794, Sept. 2020.
[39] P. Zhao, C. Gu, and D. Huo, "Two-stage coordinated risk mitigation strategy for integrated electricity and gas systems under malicious false data injections," *IEEE Transactions on Power Systems*, doi: 10.1109/TPWRS.2020.2986455
[40] F. Teng, H. Zhang, C. Luo *et al*., "Delay tolerant containment control for second-order multi-agent systems based on communication topology design," *Neurocomputing*, vol. 380, pp. 11-19, Mar. 2020.
[41] Q. Shan, J. Yan, T. Li *et al*., "Containment control of multi-agent systems with general noise based on hierarchical topology reconfiguration," *IEEE Access*, vol. 7, pp. 56826-56838, Nov. 2019.
[42] S. Zuo, F. L. Lewis, and A. Davoudi, "Resilient output containment of heterogeneous cooperative and adversarial multi-group systems," *IEEE Transactions on Automatic Control*, vol. 65, no. 7, pp. 3104-3111, Jul. 2020.
[43] J. Zhou, H. Sun, Y. Xu *et al*., "Distributed power sharing control for islanded single-/three-phase microgrids with admissible voltage and energy storage constraints," *IEEE Transactions on Smart Grid*, vol. 12, no. 4, pp. 2760-2775, Feb. 2021.
[44] H. Sun, Q. Guo, J. Qi *et al*., "Review of challenges and research opportunities for voltage control in smart grids," *IEEE Transactions on Power Systems*, vol. 34, no. 4, pp. 2790-2801, Jul. 2019.
[45] S. Golestan, J. M. Guerrero, J. C. Vasquez *et al*., "All-pass-filter-based PLL systems: linear modeling, analysis, and comparative evaluation," *IEEE Transactions on Power Electronics*, vol. 35, no. 4, pp. 3558-3572, Apr. 2020.

Jianguo Zhou received the B.S. degree in automation, and the M.S. and Ph. D. degrees in control theory and control engineering from Northeastern University, Shenyang, China, in 2011, 2013, and 2018, respectively. Since December 2018, he has been a Postdoctoral Researcher with the Tsinghua-Berkeley Shenzhen Institute (TBSI), Tsinghua Shenzhen International Graduate School (TsinghuaSIGS), Tsinghua University, Shenzhen, China. His current research interests include power electronics, distributed control and optimization with applications in microgrids, virtual power plant and Energy Internet.

Yinliang Xu received the B.S. and M.S. degrees in control science and engineering from Harbin Institute of Technology, Harbin, China, in 2007 and 2009, respectively, and the Ph.D. degree in electrical and computer engineering from New Mexico State University, Las Cruces, USA, in 2013. He is now an Associate Professor with Tsinghua-Berkeley Shenzhen Institute (TBSI), Tsinghua Shenzhen International Graduate School (SIGS), Tsinghua University, Shenzhen, China. He is an Associate Editor for the IET Renewable Power Generation, IET Smart Grid, and IET Generation, Transmission & Distribution. His research interests include distributed control and optimization of power systems, and renewable energy integration.

Lun Yang received the B.S. degree in electrical engineering from Shihezi University, Shihezi, China, in 2016, and the M.S. degree in electrical engineering from Chongqing University, Chongqing, China, in 2019. Currently, he is pursuing the Ph. D. degree in Tsinghua-Berkeley Shenzhen Institute (TBSI), Tsinghua Shenzhen International Graduate School (TsinghuaSIGS), Tsinghua University, Shenzhen, China. His research interests include convex optimization, distributionally robust optimization and their applications in power and energy systems.

Hongbin Sun received the double B.S. degrees from Tsinghua University, Beijing, China, in 1992, the Ph.D. degree from the Department of Electrical Engineering, Tsinghua University, in 1996. From September 2007 to September 2008, he was a Visiting Professor with the School of Electrical Engineering & Computer Science, Washington State University, Pullman, USA. He is now Changjiang Scholar Chair Professor in the Department of Electrical Engineering and the Director of Energy Management and Control Research Center, Tsinghua University. He is currently an IEEE Fellow and IET Fellow. He also serves as the Editor of the IEEE Transactions on Smart Grid, Associate Editor of IET Renewable Power Generation, and member of the Editorial Board of four international journals and several Chinese journals. His research areas include electric power system operation and control with specific interests on the energy management system, system-wide automatic voltage control, and energy system integration.